



Experimental Study on the Pull-Out Capacity of Blind Rivet Nuts (BRNs) Mounted on Cold-Formed Square Hollow Section Members with Different Wall Thickness

Suleyman Istemihan COSGUN^{ID}

How to cite: Cosgun, S. I. (2023). Experimental study on the pull-out capacity of blind rivet nuts (BRNs) mounted on cold-formed square hollow section members with different wall thickness. *Sinop Üniversitesi Fen Bilimleri Dergisi*, 8(2), 202-215. <https://doi.org/10.33484/sinopfbid.1366056>

Research Article

Corresponding Author
Suleyman Istemihan COSGUN
sicosgun@erzincan.edu.tr

ORCID of the Author
S.I.C: 0000-0001-5363-0688

Received: 25.09.2023
Accepted: 30.10.2023

Abstract

In this study, pull-out tests of blind rivet nuts (BRNs) mounted on cold-formed square hollow section (SHS) webs with 100×100 mm nominal cross-section dimensions and different wall thicknesses (2.0 to 5.0 mm) were performed, and the effect of different wall thicknesses and BRN thread sizes on the test results was experimentally investigated. M10 and M12 stainless steel BRNs were mounted on SHSs using a standard riveter tool, and the test elements were prepared for the experiment. Load–displacement curves and the final damage modes were obtained for each test specimen. The results show that the pull-out capacity depends on both the SHS wall thickness and rivet nut thread size. Although the pull-out capacity increased in both thread sizes with the increase in wall thickness parameters, the effect of thread size is negligible in the case of 2.5, 3.0, and 4.0 wall thickness. In addition, when a connection is created using a BRN, the design should consider the stripped thread strength in addition to the pull-out capacity.

Keywords: Blind rivet nut, square hollow section, pull-out capacity

Farklı Et Kalınlıklarına Sahip Soğuk Şekillendirilmiş Kare İçi Boş Kesitli Elemanlara Monte Edilen Kör Perçin Somunlarının (BRN'ler) Çekme Kapasitesi Üzerine Deneysel Çalışma

Erzincan Binali Yıldırım
University, Department of Civil
Engineering, Erzincan, Türkiye

Öz

Bu çalışmada, 100x100 mm nominal kesit boyutlarına sahip farklı et kalınlıklarındaki (2.0 ile 5.0 mm) soğuk şekillendirilmiş kare içi boş profil (SHS) gövdelerine monte edilen kör perçin somunlarının (BRN'ler) çekme testleri gerçekleştirilmiş olup farklı duvar kalınlıklarının ve BRN diş boyutunun test sonuçlarına etkisi deneysel olarak araştırılmıştır. M10 ve M12 paslanmaz çelik BRN'ler standart perçinleme aleti kullanılarak SHS'lere monte edilmiş ve deney için test elemanları hazırlanmıştır. Her test numunesi için yük-yer değiştirme eğrileri ve nihai hasar modları elde edilmiştir. Sonuçlar, çekme kapasitesinin hem SHS duvar kalınlığına hem de perçin somunu diş boyutuna bağlı olduğunu göstermektedir. Her iki diş boyutunda da et kalınlığı parametrelerinin artmasıyla çekme kapasitesi artmasına rağmen, 2.5, 3.0 ve 4.0 et kalınlığı durumunda diş boyutunun etkisi ihmal edilebilir düzeydedir. Ayrıca, BRN kullanılarak bir bağlantı oluşturulduğunda, tasarımda çekme kapasitesinin yanı sıra BRN'lerin dişlerinin sıyrılma mukavemeti de dikkate alınmalıdır.

Introduction

Rivet nuts, also known as blind rivet nuts (BRNs), are versatile and easy-to-use connection members used for various materials such as metals, plastics, and composite surfaces. These designs are particularly suitable for applications where access to the rear and inner sides is restricted or impossible because they make it convenient to create threaded holes from only one side of the workpiece. In recent years, the number of studies on BRNs has increased, some of which are described as follows. Heiler [1] explored the benefits and processes of flow drilling technology and thread forming as efficient and secure methods for connecting thin-walled components and hollow sections. This technology, which involves the use of a fast-rotating carbide taper mandrel to create a bush in the material, was presented as an alternative to traditional joining methods such as welding or rivet nuts. The article also detailed the process of flow drilling and its various applications, emphasizing its efficiency and reliability compared with conventional fasteners. The study highlighted the axial forces involved in flow drilling, tool design, and thread formation in sheet metal bushes. The author concluded by asserting that flow drilling technology is an economical alternative for producing sheet metal pull-throughs and subsequent thread formation, particularly for thin-walled components and hollow profiles. Hassanifard et al. [2] investigated the fatigue life of clamped rivet-nut joints under cyclic loading. They used a finite element analysis to account for the residual stress and assessed the local stresses on the joint. The results were then used to predict the fatigue life using damage models. The study also explored the stress distribution in the rivet-nut joints and the influence of the smashing size on the fatigue life of the joints. They further investigated the strain-controlled fatigue behaviors of different materials and numerically predicted the torque-to-turn value of a BRN. The study provides valuable insights into the fatigue behavior of clamped rivet-nut joints and the importance of considering both normal and shear stress components in fatigue life prediction models. Borowiecki et al. [3] conducted numerical and experimental investigations on bolted connections with BRNs. They discussed the classification of screw connections and the associated validation process. They also examined the effect of the strength of the connected elements on the strength of the connection. The study revealed that the strength of the connection is significantly lower than the values declared by a manufacturer of BRNs. Van de Velde et al. (2019) [4] conducted a numerical prediction of the torque-to-turn value of a blind rivet nut using finite element simulations. The study aimed to improve the design of blind rivet nuts by understanding their setting process. This strategy was successfully applied to two blind rivet nuts and the results were validated through experiments. Finite element models were developed to simulate the formation process of the blind rivet nuts. They observed that the strain-hardening behavior of BRNs significantly affected the accuracy of the simulation. A finite element model updating (FEMU) technique was used to optimize the strain-

hardening behavior and torque-to-turn values in the rivet joints. This study also investigated the use of finite element analysis to support the design of BRNs. They observed that the setting process could be accurately simulated, enabling the determination of the optimal setting force, hole clearance, and deformation chamber length. The study concluded that the proposed modeling strategy can predict the forming process and the associated torque-to-turn value; however, the accuracy of the model could be improved. Studziński [5] investigated the application of analytical models to understand the elastic behavior of axially loaded blind rivets in sandwich beams. The models under consideration included the Winkler, Filonenko–Borodich, and Pasternak models. The models were validated using laboratory pull-out tests. They observed that the ultimate capacity of the rivets ranged from 240 to 300 N. While all models accurately depicted the elastic range of the mechanical response, they tended to overestimate the displacement of the face slightly. The study suggested that future research could benefit from a 2D model to better understand the mechanical response of a blind rivet pull-out from a sandwich panel facing. Van de Velde et al. (2022) [6] studied the impact of installing a BRN in a CFRP on the integrity of the plate material. The study used scanning electron microscopy (SEM) to visualize the damage induced by setting a BRN with two different setting forces. The study observed that the quasi-static strength was hardly influenced after installing the BRN when loading the laminate in the “0° orientation” (transverse fibers are dominant). The researchers hypothesized that the through-thickness stress reduces the severity of the local stress state, thus reducing local damage risks and counteracting the possible detrimental effects of damage. However, when loading the laminate in the “90° orientation” (longitudinal fibers are dominant), the quasi-static test indicated that the strength was reduced after installing the BRN. The researchers assumed that the damage to the outer layers, where the fibers were oriented in the loading direction, was responsible for the observed strength reduction. The main objective of a study by Van de Velde et al. (2023) [7] was to investigate the influence of the setting force on the static strength of BRNs embedded in carbon fiber-reinforced plastic (CFRP). The study also investigated the behavior of BRNs in CFRP laminates and the effect of the setting force on the stress state within the laminate and the strength of the joint. The findings of the study revealed that the setting force significantly influences the stress state within the laminate, thereby enhancing its static mechanical strength. The size of the BRN and the setting force are crucial factors affecting the strength of the joint. The study also observed that if no visible damage is observed in the load-carrying layers, the installation of the BRN tends to improve the static performance of the joint. However, if visible damage is induced during the BRN installation, the static strength of the joint is reduced. The push-through resistance is minimally affected by the setting force of the BRN. The study provided valuable insights into the effects of BRN installation on CFRP composites and underscored the importance of optimizing the setting force to improve performance. Kim et al. [8] investigated the impact of the clamping angle on the fastening force in BRN fastening. M6 BRNs were used in the tests. They found that as the clamping angle increases, the fastening force decreases, suggesting a clamping angle of less than 3° is optimal. The

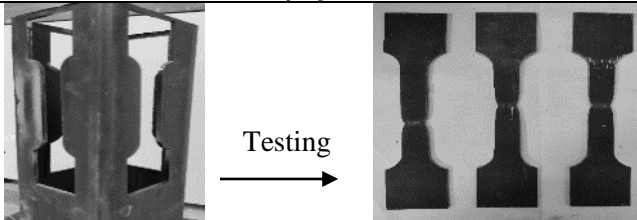
study concluded by emphasizing the need for further research on BRN geometry optimization and the development of jigs for manual fastening. Gu et al. [9] conducted a study on the design optimization of M8 BRN using finite element analysis. The research primarily focused on the impact of the shaft shape of the BRN on the fastening process. The study concluded that shaft thickness and height are the most significant design variables, influencing the gap and load on the plate. The coefficient of friction was found to have a minimal effect on the maximum effective stress and the average plate load. The main objective of this study was to conduct preliminary experimental studies to determine the behavior and pull-out capacity of BRN under load and to investigate the effect of different wall thicknesses of square hollow sections (SHSs) on the behavior and capacity when BRN is used in lightweight and particularly hollow steel structures. Additionally, the effect of BRN sizes (M10 and M12) on pull-out capacity was investigated.

Experimental Study

Tensile Tests

Tensile tests were performed according to ASTM A370-14 [10] to determine the material properties of cold-formed SHSs with five different wall thicknesses considered within the scope of the study. The results are summarized in Table 1.

Table 1. Summary of the tensile test results



Sample	Width (mm)	Nominal thickness (mm)	Measured thickness (mm)	Elastic modulus (GPa)	Nominal yield strength (MPa)	Nominal tensile strength (MPa)
SHS 100x100x5.00	20.00	5.00	4.95	195	280	378
	20.01			200	280	365
	20.02			196	283	375
SHS 100x100x4.00	19.99	4.00	3.85	186	352	412
	19.98			189	350	407
	20.00			193	348	410
SHS 100x100x3.00	14.00	3.00	2.85	-	295	384
	13.98			-	289	379
	13.98			-	296	381
SHS 100x100x2.50	14.00	2.50	2.35	196	308	397
	13.98			-	308	384
	13.99			199	310	398
SHS 100x100x2.00	14.00	2.00	1.95	-	338	462
	13.97			-	335	463
	13.98			-	336	461

Properties of the Test Specimens

Each SHS test specimen was 200 mm in length, and 13 mm and 16 mm holes were drilled in its middle, as specified in the manufacturer's assembly instructions, and mounted. The same settling force was applied as that of the standard riveter tool, regardless of the thickness of the mounted SHS in all test elements. A schematic of the blind-rivet nut installation is shown in Figure 1. The dimensions of the BRNs are listed in Table 2.

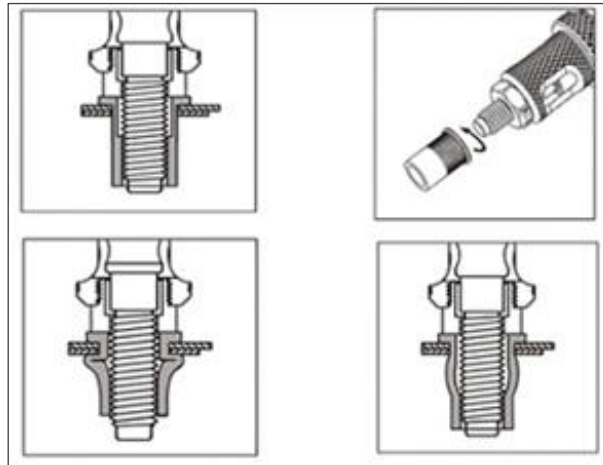
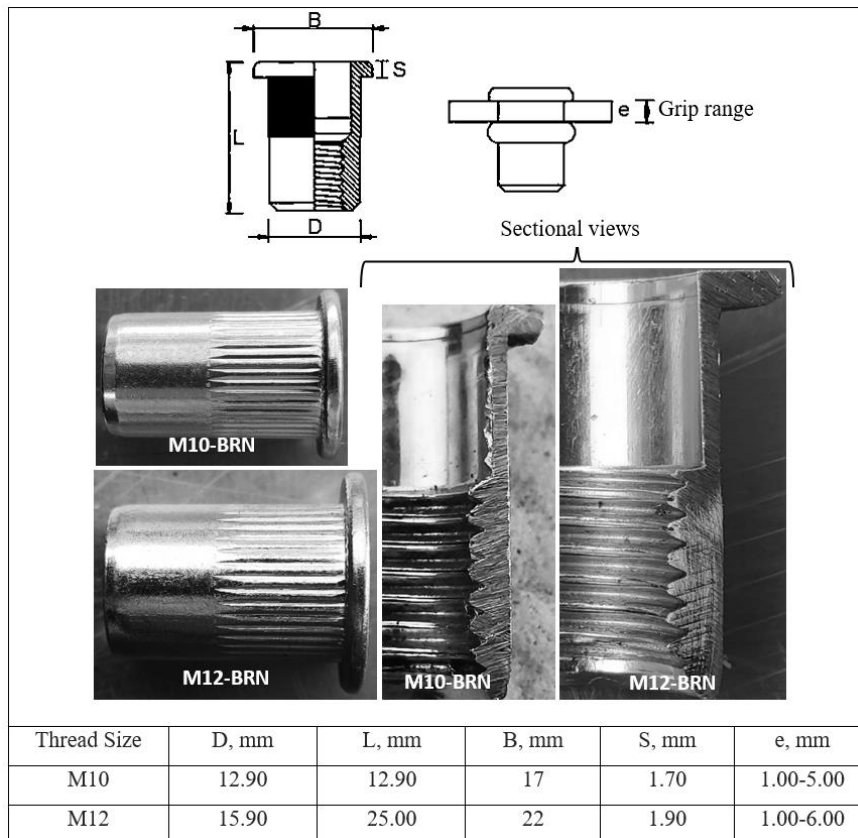


Figure 1. Schematic of the installation stages of a BRN [11]

Table 2. Measured dimensions of the BRNs



Loading Scheme and Measuring Instruments

The specimens were tested using a test setup with two 50-kN hydraulic jacks for monotonic pull loading. Before the loading process was initiated, a test specimen was positioned at the center of the loading setup to ensure concentric axial pulling loading, and the possible rotation of the loading plate was controlled with a digital angle meter placed on the loading plate during the experiment. A consistent loading protocol was applied to all the specimens. The loading continued monotonically until the rivet nut was removed from the mounted SHS. Although the loading rate could not be applied as standard in all experiments, it could be applied approximately between 0.6 and 1.00 mm/sec. A linear variable differential transformer (LVDT) was used to measure the displacement in the loading direction from the loading plate. Data were acquired using a Testbox 1001 data acquisition system (Ankara, Türkiye). A photograph of the test setup is shown in Figure 2.

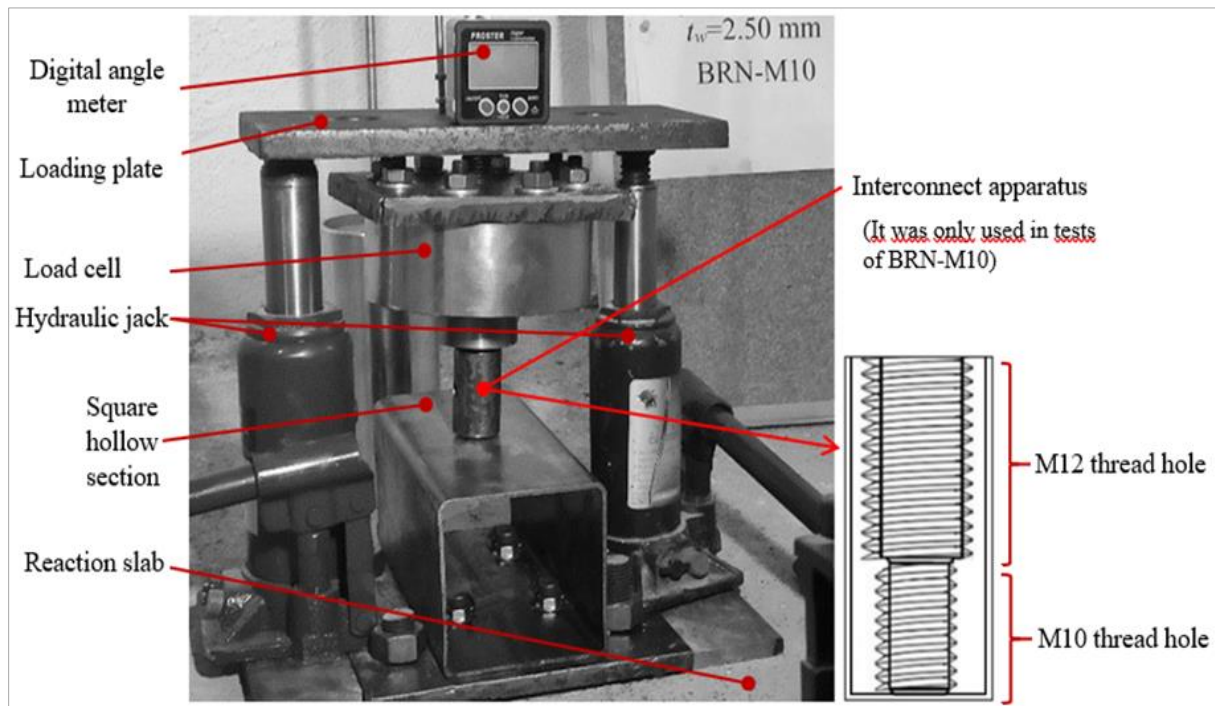


Figure 2. Test setup with instrumentation

Results and Discussions

This study investigated the behavior and ultimate pull-out capacities of single M10 and M12 stainless-steel BRNs mounted on the walls of ten 200 mm-long SHSs with different wall thicknesses under monotonic tensile loading. The summary of the test results and load–displacement curves are presented in Figure 3 and Table 3, respectively. When the initial stiffness was evaluated, the differences in the initial stiffness plots obtained when M10 and M12-sized BRNs mounted on SHSs with different wall thicknesses were tested were negligible (Table 3).

Table 3. Summary of the test results

Specimen ID	Nominal SHS wall thickness, mm	Used BRN	Pull-out capacity, kN	Initial stiffness, kN/mm	Rivet nut hole diameter after test, mm	Global section deformation, mm
S1	2.00	M10	11.37	1.10	16.50	107.30
S2	2.50		14.10	1.25	15.90	101.80
S3	3.00		17.42	1.76	15.80	100.80
S4	4.00		25.40	5.55	13.40	100.00
S5	5.00		30.00	8.38	13.20	100.00
S6	2.00	M12	13.75	1.11	20.30	119.00
S7	2.50		14.15	1.26	19.70	104.50
S8	3.00		17.70	1.80	18.80	101.20
S9	4.00		26.50	5.60	16.80	100.00
S10	5.00		35.84	8.40	16.70	100.00

This is because the behavior of the initial stiffness in the first phase depends on the geometry (wall thickness) and material properties of the SHS wall mounted on it rather than the BRN sizes. Thus, in the experiments in which both BRNs were used, the initial stiffness increased with an increase in the SHS wall thickness.

This is because the behavior of the initial stiffness in the first phase depends on the geometry (wall thickness) and material properties of the SHS wall mounted on it rather than the BRN sizes. Thus, in the experiments in which both BRNs were used, the initial stiffness increased with an increase in the SHS wall thickness. Additionally, as shown in Figure 4, an approximately linear relationship was observed between SHS wall thickness and BRN pull-out capacity for both BRN sizes.

In other words, the grip strength of M12 BRN was approximately 21% more than M10 at a wall thickness of 2.0 mm. The reason for the difference in the pull-out capacities obtained from M10 and M12 BRNs for 5 mm wall thickness was that when M10 was used, capacity loss occurred owing to stripped thread damage of BRN (Figure 7). When M12 was used, the damage was a combination of rupturing of the BRN neck and removal of the BRN from the SHS wall (Figure 8). Before the stripped thread damage to the BRN occurred, the loss of capacity was due to SHS wall deformation. This was because the stripped thread strength was approximately 20% higher in the M12 threads than in the M10 BRN (see [12, 13]). Therefore, when M12 was used, the increase in capacity compared with M10 was approximately 20%.

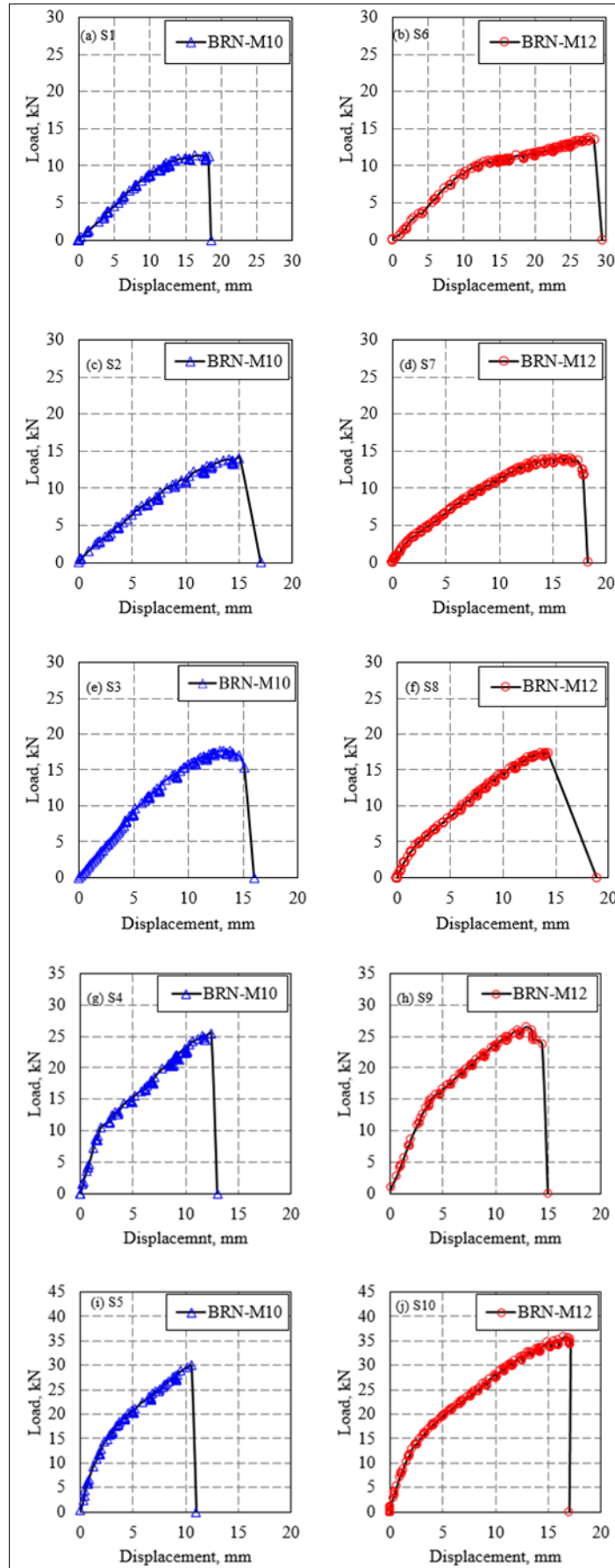


Figure 3. Load–displacement curves

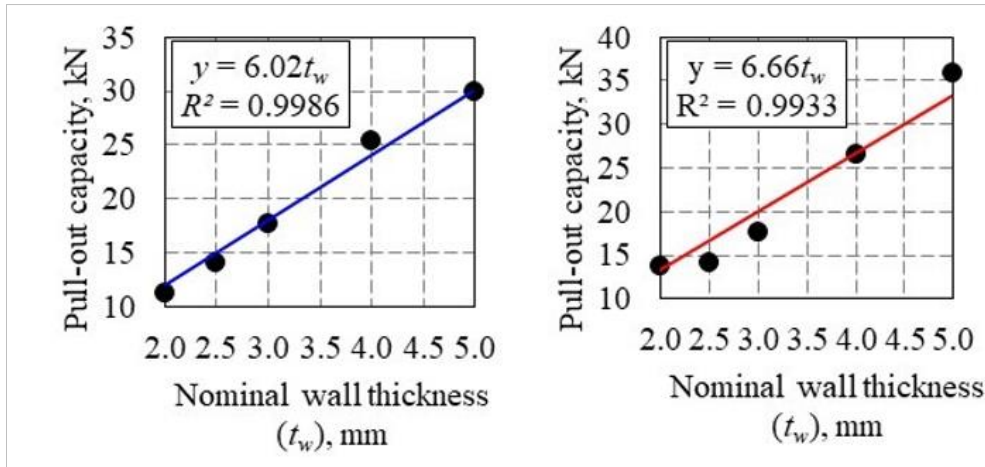


Figure 4. Relationship between wall thicknesses and pull-out capacity

When pull-out capacities were evaluated, in cases in which both M10 and M12 rivet nuts were used, the capacity increased with the increase in the SHS wall thickness, as in the initial stiffness. Additionally, the findings showed that the effect of BRN size was negligible when the wall thickness was 2.50, 3.00, and 4.00 mm (Figure 5).

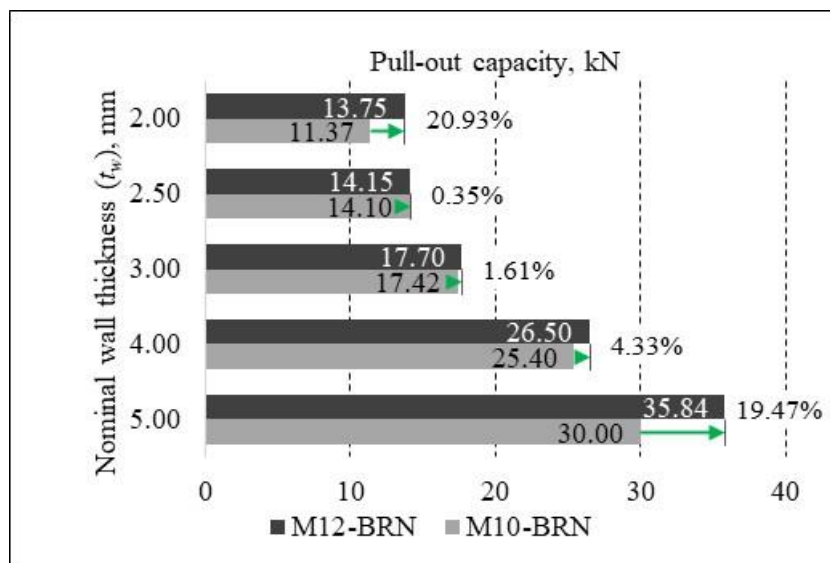


Figure 5. Comparison of pull-out capacities

However, for wall thicknesses of 2.00 and 5.00 mm, the increases in pull-out capacity were 21% and 19.5%, respectively. Unlike at other thicknesses, the effect of the BRN size was more pronounced at these values. The effect of M10 and M12 on the load–displacement relationship was negligible up to a displacement of approximately 18 mm at a wall thickness of 2 mm. However, after this displacement value, when the M12 BRN was used, the final capacity increased as the load was transferred to the SHS wall through the rivet nut. This caused the global deformation in the measured SHS to be greater when the M12 BRN was used than when the M10 SHS was used (Figure 6).

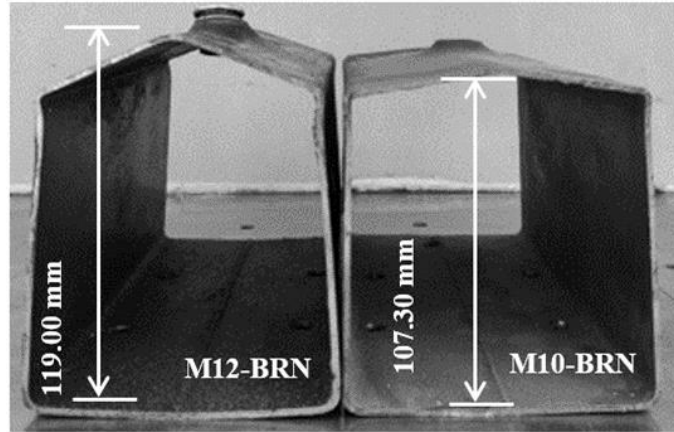


Figure 6. Global deformation of S1(right) and S6 (left)

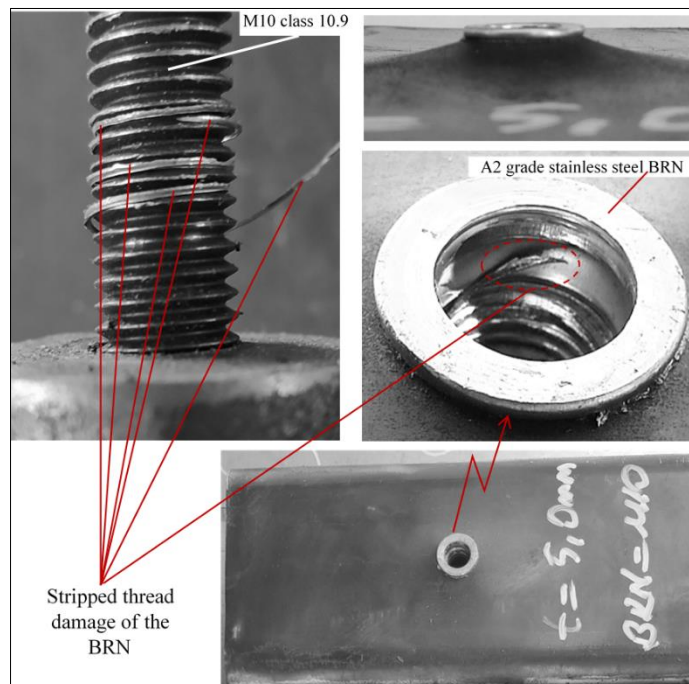


Figure 7. Ultimate damage modes of S5 ($t_w=5.00$ mm and BRN-M10)



Figure 8. Failure mode in the BRN of S10 ($t_w=5.00$ mm and BRN-M12)

Photographs of the damage modes obtained as a result of all tests are presented in Figure 9. When the damage modes were evaluated, as the SHS wall thickness increased at both BRN thread sizes, the damage to the SHS wall transitioned from global sectional and local conical deformation to only local conical damage and excessive BRN damages (Figure 9, Figure 10).

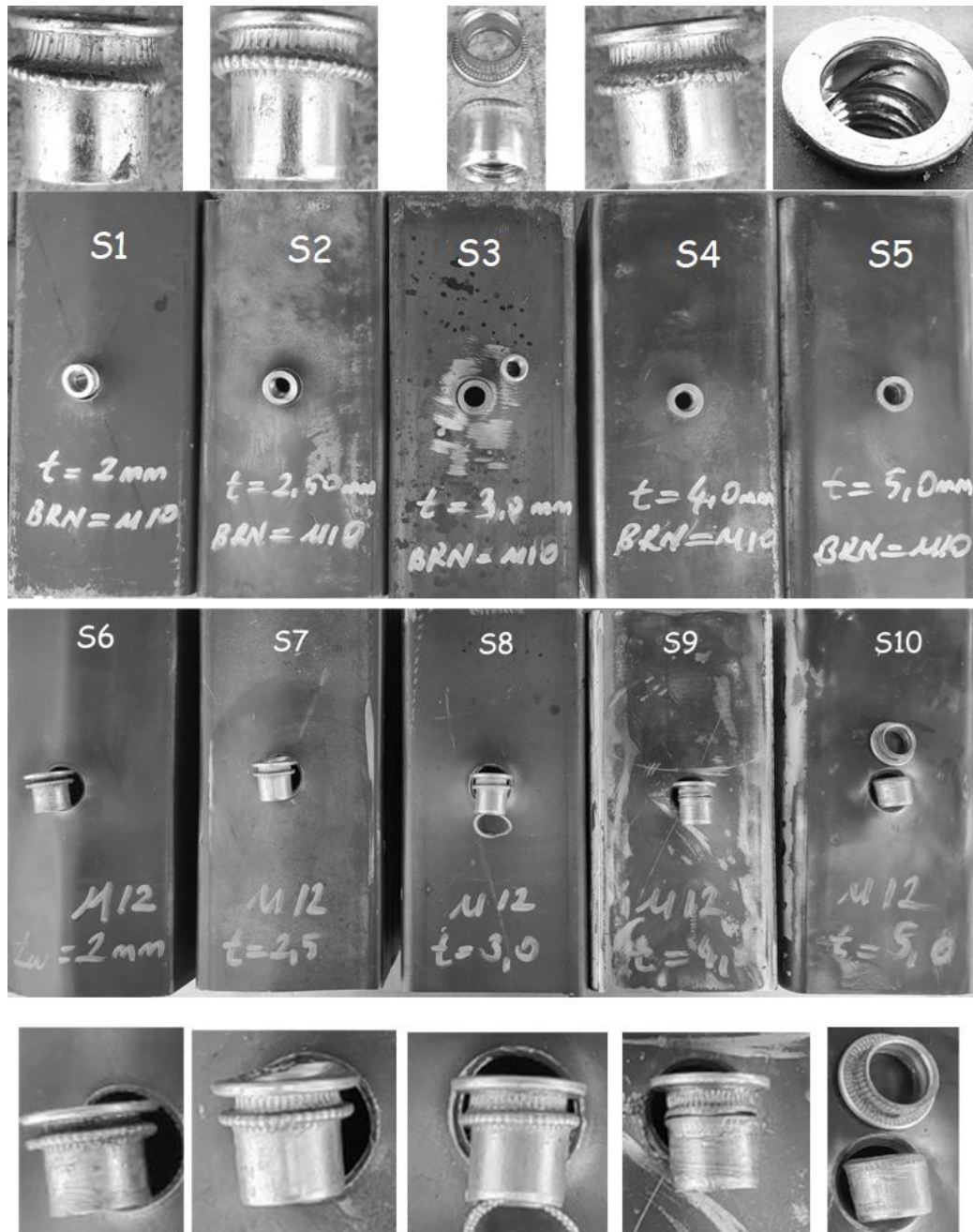


Figure 9. Photographs of final damage modes of all experimental elements

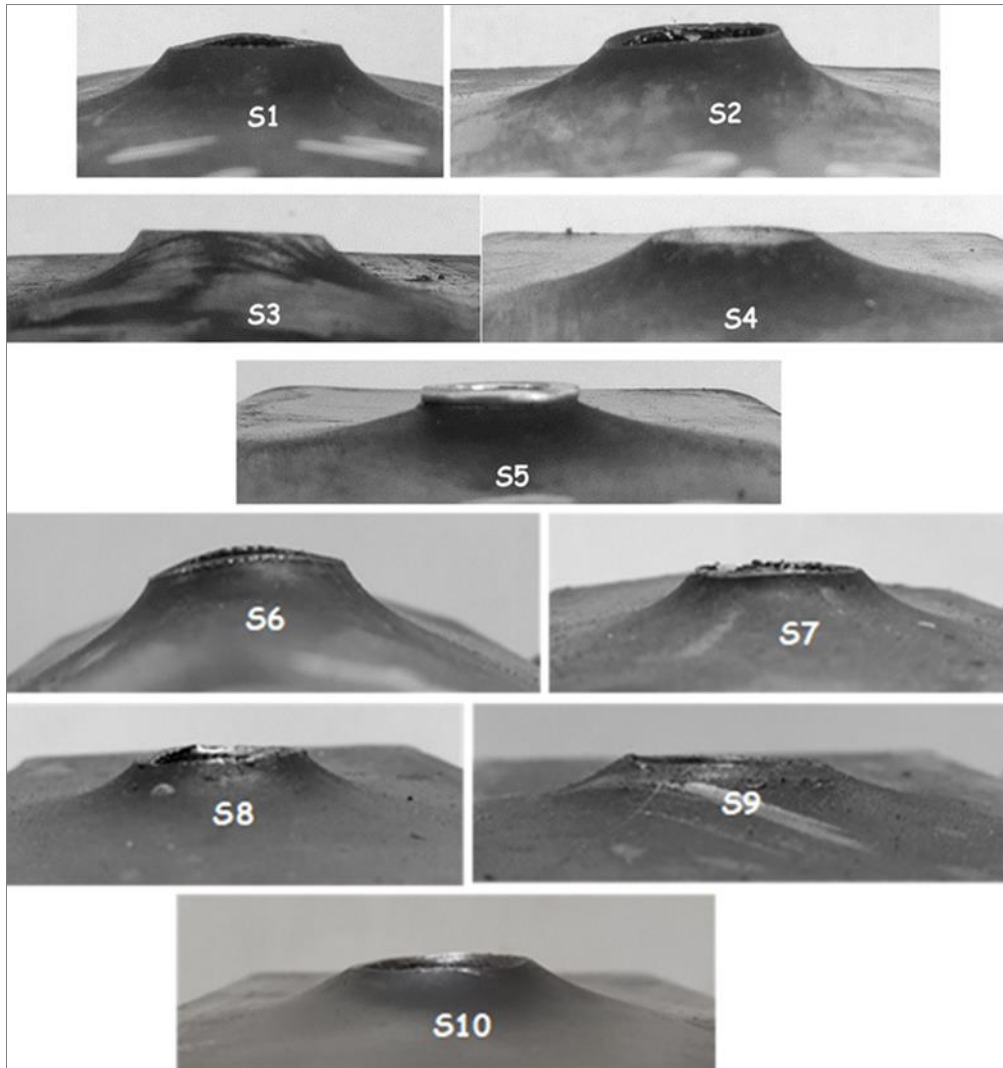


Figure 10. Conical deformation modes of the SHS wall

Conclusions

In this study, pull-out tests of M10 and M12 stainless steel BRNs mounted on cold-formed square hollow section (SHS) bodies with 100×100 mm nominal cross-section dimensions and different wall thicknesses (2.0 to 5.0 mm) were performed, and the effect of different wall thicknesses and BRN thread sizes on the test results was experimentally investigated. The results of the study are summarized as follows:

- The initial stiffness depends largely on the SHS wall properties than on BRN size (M10 or M12).
- Pull-out capacity increases with thicker SHS walls regardless of BRN size.
- BRN size has a minimal impact on pull-out capacity for 2.50, 3.00-, and 4.00-mm walls. For 2.00- and 5.00-mm walls, M12 BRNs offer significantly higher pull-out capacity (21% and 19.5% more) than M10 BRNs.

- The effect of BRN size on the load–displacement relationship is negligible up to an 18-mm displacement for 2.00 mm walls. Beyond 18 mm, M12 BRNs provide approximately 21% higher grip strength than M10 BRNs for 2.00 mm walls.
- The difference in the pull-out capacities for 5-mm walls is due to M10 BRNs undergoing stripped thread damage, whereas M12 BRNs undergo neck rupture and BRN removal.
- M12 BRNs have approximately 20% higher stripped thread strength than M10 BRNs, resulting in increased pull-out capacity.
- When the damage modes were assessed, the damage to the SHS wall changed from global sectional and local conical deformation to only local conical damage and excessive BRN damage as the SHS wall thickness increased at both BRN thread sizes.

This study was conducted considering the limited number of test specimens and the BRN thread sizes. It should be particularly noted that these results are not generalizable, and the investigation scope should be expanded by increasing the number of test specimens to have a deeper insight into the subject.

Acknowledgments -

Funding/Financial Disclosure This research did not receive any specific grant from funding agencies in the public, commercial, or not-for-profit sectors.

Ethics Committee Approval and Permissions The study does not require ethics committee permission or any special permission.

Conflict of Interests The author declares that they have no known competing financial interests or personal relationships that could have appeared to influence the work reported in this paper.

Authors Contribution The author read and approved the final manuscript.

References

- [1] Heiler, R. (2019). Flow drilling technology and thread forming - an economical and secure connection in hollow sections and thin-walled components. *E3S Web of Conferences*, 97, 06033. <https://doi.org/10.1051/e3sconf/20199706033>
- [2] Hassanifard, S., Adibeig, M., Mohammadpour, M., & Varvani-Farahani, A. (2019). Fatigue life of axially loaded clamped rivet-nut joints: Experiments and analyses. *International Journal of Fatigue*, 129, 105254. <https://doi.org/10.1016/j.ijfatigue.2019.105254>
- [3] Borowiecki, C., Iluk, A., Krysiński, P., Rusiński, E., & Sawicki, M. (2019, January 1). *Numerical and Experimental Investigation of Bolted Connections with Blind Rivet Nuts*. Lecture Notes in Mechanical Engineering. https://doi.org/10.1007/978-3-030-04975-1_11
- [4] Van de Velde, A., Coppieters, S., Maeyens, J., Wevers, M., & Debruyne, D. (2019). On the numerical prediction of the torque-to-turn-value of a blind rivet nut. *International Journal of Material Forming*, 13(1), 127–141. <https://doi.org/10.1007/s12289-019-01476-5>

- [5] Studziński, R. (2021). Analytical models of axially loaded blind rivets used with sandwich beams. *Energies*, 14(3), 579. <https://doi.org/10.3390/en14030579>
- [6] Van de Velde, A., Ivens, J., Maeyens, J., & Coppieters, S. (2022). The effect of the setting force on the fatigue resistance of a blind rivet nut set in CFRP. *Key Engineering Materials*, 926, 1498–1504. <https://doi.org/10.4028/p-4w99oa>
- [7] Van de Velde, A., Maeyens, J., Ivens, J., & Coppieters, S. (2023). The effect of the setting force on the static strength of a blind rivet nut set in CFRP. *Composite Structures*, 307, 116640. <https://doi.org/10.1016/j.compstruct.2022.116640>
- [8] Kim, C., Gu, B., Yi, S., Choi, J. M., & Hong, S. (2020). Accurate Fastening of Blind Rivet Nuts: A Study. *Transactions of Materials Processing*, 29(6), 331–337. <https://doi.org/10.5228/KSTP.2020.29.6.331>
- [9] Gu, B., Choi, J. M., & Hong, S. (2020). Design Optimization of M8 Blind Rivet Nut Geometry using Finite Element Analysis. *Transactions of Materials Processing*, 29(3), 157–162. <https://doi.org/10.5228/KSTP.2020.29.3.157>
- [10] American Society for Testing and Materials. (2014). Standard Test Methods and Definitions for Mechanical Testing of Steel Products, ASTM A370-14.
- [11] *Alcoa Marson Rivet Nut Installation Tool Kit with Inch Mandrels*. (n.d.). DMSeeleysTools.com. <https://dmseeleystools.com/alcoa-marson-rivet-nut-installation-tool-kit-with-inch-mandrels/>
- [12] Beek, A. van. (2019). *Advanced Engineering Design: Lifetime Performance and Reliability*. TU Delft.
- [13] Juvinall, R. C., & Marshek, K. M. (2020, June 23). *Fundamentals of Machine Component Design*. John Wiley & Sons.